JACS
JOURNAL OF THE AMERICAN CHEMICAL SOCIETY
Article
pubs.acs.org/JACS

Simultaneous Dual Protein Labeling Using a Triorthogonal Reagent

Mohammad Rashidian,[†,‡] Sidath C. Kumarapperuma,[†,§] Kari Gabrielse,[§] Adrian Fegan,[§] Carston R. Wagner,*[,§] and Mark D. Distefano*[,‡]

[‡]Department of Chemistry, and [§]Department of Medicinal Chemistry, University of Minnesota, Minneapolis, Minnesota 55455, United States

Supporting Information

ABSTRACT: Construction of heterofunctional proteins is a rapidly emerging area of biotherapeutics. Combining a protein with other moieties, such as a targeting element, a toxic protein or small molecule, and a fluorophore or polyethylene glycol (PEG) group, can improve the specificity, functionality, potency, and pharmacokinetic profile of a protein. Protein farnesyl transferase (PFTase) is able to site-specifically and quantitatively prenylate proteins containing a C-terminal CaaX-box amino acid sequence with various modified isoprenoids. Here, we describe the design, synthesis, and application of a triorthogonal reagent, **1**, that can be used to site-specifically incorporate an alkyne and aldehyde group simultaneously into a protein. To illustrate the capabilities of this approach, a protein was enzymatically modified with compound **1** followed by oxime ligation and click reaction to simultaneously incorporate an azido-tetramethylrhodamine (TAMRA) fluorophore and an aminooxy-PEG moiety. This was performed with both a model protein [green fluorescent protein (GFP)] as well as a therapeutically useful protein [ciliary neurotrophic factor (CNTF)]. Next, a protein was enzymatically modified with compound **1** followed by coupling to an azido-bis-methotrexate dimerizer and aminooxy-TAMRA. Incubation of that construct with a dihydrofolate reductase (DHFR)−DHFR−anti-CD3 fusion protein resulted in the self-assembly of nanoring structures that were endocytosed into T-leukemia cells and visualized therein. These results highlight how complex multifunctional protein assemblies can be prepared using this facile triorthogonal approach.

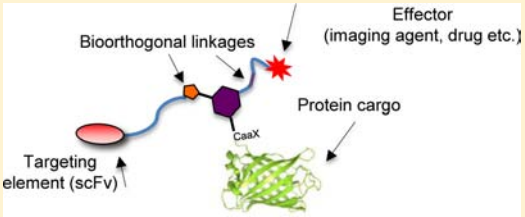

INTRODUCTION

Over the course of the past decade, bioorthogonal chemical methods have been developed for the site-specific chemical modification of proteins and used to alter their properties and function.[1−7] For example, fluorophores can be site-specifically attached to proteins as a biophysical or cellular localization tool, while protein−polymer conjugation is a well-established method for modulating the *in vivo* behavior of proteins.[8−11] In addition, a number of groups have reported bioorthogonal approaches for the construction of bifunctional protein assemblies. Schultz and co-workers coupled two antibody Fab fragments via an alkyne−azide cycloaddition click reaction using non-natural mutagenesis techniques.[12] Bertozzi and co-workers used an enzymatic formyl generating strategy[13] to generate an aldehyde that was then converted to a cyclooctyne- or azide-functionalized protein via oxime formation followed by reaction with other azide-modified peptides or proteins. Ploegh and co-workers used a variation of sortagging to create N−N and C−C protein conjugates by preparing pairs of azide- and alkyne-containing proteins that were then linked via click reactions.[14] In the above examples, proteins equipped with a single bioorthogonal group were modified with a second small molecule, polymer, or protein bearing a complementary functional group.

Recently, progress toward the introduction of multiple functional groups into proteins has also been made. Wu and co-workers developed a strategy for site-specific two-color labeling of a Rab GTPase for fluorescence resonance energy transfer (FRET) applications by applying chemoselective native chemical ligation and oxime ligation simultaneously.[15] A C-terminal oxime was generated via expression of a C-terminal thioester, while an N-terminal cysteine (for subsequent ligation) was revealed by Tobacco etch virus (TEV)-catalyzed proteolysis. In other work, Schultz and co-workers developed a method for site-specific dual labeling of proteins for FRET analysis based on the use of selective cysteine alkylation combined with non-natural amino acid incorporation of a ketone moiety.[16] Park and co-workers successfully incorporated two unnatural amino acids bearing ketone and alkyne groups into a protein for analysis of protein dynamics using a related nonsense suppression approach.[17] Very recently, Chen and co-workers designed and synthesized bifunctional sialic acid analogues containing azide and alkyne moieties for incorporation of two distinct chemical reporters into cellular sialylated glycans for FRET imaging.[18] While useful, that method is limited to sialylated cell surface glycans and requires metabolic activation of the bifunctional sialic acid analogue to the corresponding cytosine monophosphate (CMP) sugar prior to incorporation.

Previously, our group and others have exploited the high specificity of protein farnesyl transferase (PFTase) to site-

Received: April 16, 2013
Published: October 17, 2013

 © 2013 American Chemical Society dx.doi.org/10.1021/ja403813b | J. Am. Chem. Soc. 2013, 135, 16388−16396

specifically modify proteins.[19−22] PFTase catalyzes the transfer of an isoprenoid group from farnesyl diphosphate (FPP; Figure 1A) to a cysteineyl sulfur atom present in a tetrapeptide

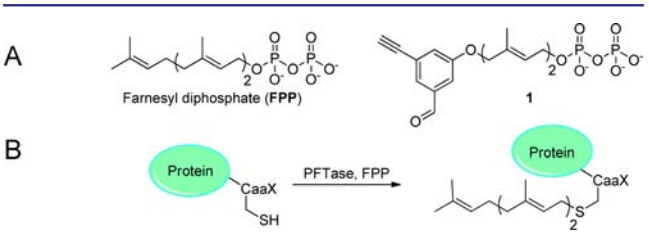

Figure 1. (A) Structures of FPP and compound **1**. (B) Schematic representation of farnesylation reaction with a protein containing a CaaX box at its C terminus.

sequence (denoted as a CaaX box) positioned at the C terminus of a protein (Figure 1B). Importantly, CaaX-box sequences, such as CVIA, can be appended to the C termini of many proteins, rendering them efficient substrates for PFTase. Because PFTase can tolerate many simple modifications to the isoprenoid substrate,[23−26] it can be used to introduce a variety of functional groups into proteins; PFTase and some bioorthoganol substrates are already commercially available. Previously, we have showed that aldehyde-containing FPP analogues and alkyne-containing FPP analogues can be successfully incorporated into proteins using this strategy.[19,23,27] Consequently, we envisioned that enzymatic incorporation of a substrate analogue containing both alkyne and aldehyde functionality could be used to generate proteins with two distinct orthogonal functional groups for subsequent elaboration. This approach would enable site-specific and simultaneous protein modification with two orthogonal groups, which can be used to improve the specificity, functionality, potency, and pharmacokinetic profile of the protein. In contrast to the method reported by Chen and co-workers noted above, our approach requires no metabolic incorporation and can be applied to essentially any protein that can be successfully expressed with a C-terminal CaaX-box fusion.[18] To implement this strategy, a triorthogonal molecule (**1**) was designed that contained an allylic diphosphate, rendering it a substrate for PFTase, as well as an aldehyde and alkyne. The compound was synthesized in nine steps and shown to be a substrate. Next, to showcase the utility of this molecule for multiple modification reactions on a single polypeptide, it was used to selectively functionalize a protein with both fluorophore and polyethylene glycol (PEG) groups. Those two groups were chosen as examples because fluorophores can act as biophysical or cellular localization tools, while PEG moieties are useful for modulating the pharmacokinetics of protein-based drugs. To further highlight the capabilities of this strategy, a larger multifunctional nanoscale construct was prepared. Compound **1** was used to prepare a protein labeled with a fluorophore and a chemical dimerizer, which was then used to self-assemble a nanoring structure that was targeted to and readily internalized by T-leukemia cells. This illustrates the power of this triorthogonal strategy for self-organization of protein molecules into higher order structures, which is an integral part of living cells.

EXPERIMENTAL SECTION

Docking. To model compound **1** in the active site of PFTase (PDB file 1JCR), docking was performed using Glide (version 5.5, Schrodinger). The PFTase crystal structure was prepared using the default settings in the protein preparation wizard as part of the Maestro 9.0 package. A receptor grid large enough to encompass the entire binding site for compound **1** was generated from the prepared PFTase enzyme. A standard precision docking parameter was set, and 100 ligand poses per docking were run. The 20 top poses with the lowest docking score were then further subjected to postdocking minimization. The conformations with overall lowest energy were chosen for display for each probe. The Glide (version 5.5) and Maestro (version 9.0) software used in docking studies was licensed from Schrodinger, LLC (New York).

Enzymatic Studies of FPP Analogue 1 Using a Continuous Fluorescence Assay. Enzymatic reaction mixtures contained tris(hydroxymethyl)aminomethane (Tris)·HCl (50 mM, pH 7.5), $MgCl_2$ (10 mM), $ZnCl_2$ (10 μM), dithiothreitol (DTT) (5.0 mM), 2.4 μM *N*-dansyl-GCVIA (**2**), 0.040% (w/v) *n*-dodecyl-β-D-maltoside, PFTase (80 nM), and varying concentrations of compound **1** (0−50 μM), in a final volume of 250 μL. The reaction mixtures were equilibrated at 30 °C for 1 min, initiated by the addition of PFTase, and monitored for an increase in fluorescence (λ_{ex}, 340 nm; λ_{em}, 505 nm) for approximately 20 min. The initial rates of formation of products were obtained as slopes in IU/min using least-squares analysis. Corrections were applied to all of the rate calculations based on the difference between the fluorescence intensity of the prenylated product and the starting peptide. Assuming 100% conversion, the difference corresponds only to the fluorescence of the total amount of the product. The slope was then divided by the fluorescence difference followed by multiplying by the total concentration of peptide (2.4 μM), which then gives the rate of formation of product in μM/s. It should be noted that the K_M values reported here are actually apparent K_M values, because the measurements were performed in only a single peptide concentration. The data were fit to a Michaelis−Menten model ($V = (([E_0]k_{cat}[S])/(K_M + [S]))$ using a nonlinear regression program, to determine k_{cat} and K_M (see Figure S4 of the Supporting Information).

Enzymatic Incorporation of Compound 1 into Green Fluorescent Protein (GFP)−CVIA (3).[27] Enzymatic reaction mixtures (10 mL) contained Tris·HCl (50 mM, pH 7.5), $MgCl_2$ (10 mM), KCl (30 mM), $ZnCl_2$ (10 μM), DTT (5.0 mM), compound **7** (2.4 μM), compound **1** (30−50 μM), and PFTase (80−200 nM). After incubation at 30 °C for 4 h, the reaction mixture was concentrated using an Amicon Centriprep centrifugation device (10 000 MW cutoff). Next, excess of compound **1** was removed through a NAP-5 (Amersham) column using Tris·HCl (50 mM, pH 7.5) as the eluant. The subsequent protein concentration was calculated by ultraviolet (UV) absorbance at 488 nm (ε = 55 000 M^{-1} cm^{-1}).

Initial Evaluation of Bifunctionalized GFP (4) with Aminooxy-dansyl (S10) and Azido-tetramethylrhodamine (TAMRA) (S11). *Coupling Reaction between Bifunctionalized GFP (4) with Aminooxy-dansyl (S10).* Aminooxy-dansyl (**S10**) [3.2 μL of 10 mM solution in dimethyl sulfoxide (DMSO)] was added to 42 μL of compound **4** (stock solution of 60 μM in 0.1 M phosphate buffer at pH 7.0). Phosphate buffer (1 M, 2.5 μL, pH 7.0) was added, and the reaction was initiated by adding 40 mM *m*-phenylendiamine as a catalyst and allowed to proceed for 2 h at room temperature. The mixture was then purified by a NAP-5 column to remove excess dye. Liquid chromatography−mass spectrometry (LC−MS) analysis of the sample showed only oxime-ligated protein, and no free aldehyde was detected, suggesting that the reaction had proceeded to completion. A gradient of 0−100% solvent A (H_2O, 0.1% HCO_2H) to B (CH_3CN, 0.1% HCO_2H) in 25 min was used for the LC−MS analysis.

Coupling Reaction between Bifunctionalized GFP (4) with Azido-TAMRA (S11). Azide-TAMRA (**S11**) (7 μL of 2.2 mM solution in DMSO) was added to 100 μL of compound **4** [stock solution of 40 μM in phosphate buffer (PB)]. $CuSO_4$ (1 mM), tris(2-carboxyethyl)-phosphine (TCEP) (1 mM), and tris(benzyltriazolylmethyl)amine (TBTA) (100 μM) were added, and the reaction was allowed to proceed for 3 h. LC−MS analysis of the sample showed the presence of both the clicked protein **4a** and the free alkyne protein **4**. The ratio of free alkyne protein **4** to its respective clicked product **4a** was ∼2,

dx.doi.org/10.1021/ja403813b | J. Am. Chem. Soc. 2013, 135, 16388−16396

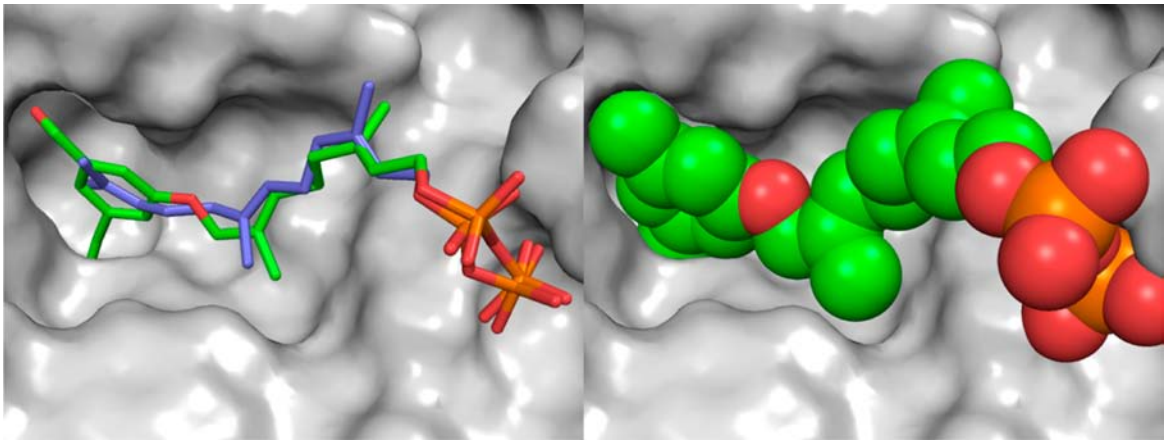

Figure 2. Docked structure of triorthogonal reagent **1** bound to PFTase. (Left) Docked structure of compound **1** superimposed on the structure of FPP bound to PFTase (obtained from X-ray crystallographic data; PDB file 1JCR). FPP is shown in blue. Compound **1** is shown in green (C), red (O), and orange (P). The protein surface is shown in gray. (Right) Docked structure of compound **1** bound to PFTase in a space-filling CPK representation (same color scheme).

indicating that only ~35% completion of the click reaction had been achieved within this time and range of reactant concentrations. The reaction was repeated using 50% more azido-TAMRA (**S11**) (225 μM) and was allowed to proceed for 16 h. LC–MS analysis of the reaction mixture showed >95% conversion of compound **4** to its respective clicked product **4a**. A gradient of 0–100% solvent A (H_2O, 0.1% HCO_2H) to B (CH_3CN, 0.1% HCO_2H) in 25 min was used for the LC–MS analysis.

*Simultaneous Coupling Reaction between Bifunctionalized GFP (**4**) with Azido-TAMRA **S11** and Aminooxy-dansyl **S10**.* Azido-TAMRA (**S11**) (7 μL of 2.2 mM solution in DMSO) and aminooxy-dansyl (**S10**) (7 μL of 10 mM solution in DMSO) were added to 100 μL of compound **4** (stock solution of 40 μM in PB). $CuSO_4$ (1 mM), TCEP (1 mM), TBTA (100 μM), and *m*-phenylenediamine (mPDA) (40 mM) were added, and the reaction was allowed to proceed for 15 h. LC–MS analysis of the sample showed >90% conversion of the click reaction and >99% oxime ligation on the protein. A gradient of 0–100% solvent A (H_2O, 0.1% HCO_2H) to B (CH_3CN, 0.1% HCO_2H) in 25 min was used for the LC–MS analysis.

Modification of Bifunctionalized GFP (4) with Azido-TAMRA (S11) and Aminooxy-PEG (S12). Azido-TAMRA (**S11**) (7 μL of 2.2 mM solution in DMSO) and aminooxy-PEG (**S12**) (3 kDa, from Quanta BioDesign, Ltd.) (2 μL of 30 mM solution in DMSO) were added to 100 μL of compound **4** (stock solution of 40 μM in PB). $CuSO_4$ (1 mM), TCEP (1 mM), TBTA (100 μM), and mPDA (40 mM) were added, and the reaction was allowed to proceed for 15 h. Sodium dodecyl sulfate–polyacrylamide gel electrophoresis (SDS–PAGE) analysis of the reaction revealed highly selective and almost complete (>95%) conversions for both oxime and click reactions.

Prenylation of CNTF–CVIA (5) with Compound 1. Enzymatic reaction mixtures (20 mL) contained Tris·HCl (50 mM, pH 7.5), $MgCl_2$ (10 mM), KCl (30 mM), $ZnCl_2$ (10 μM), DTT (5.0 mM), CNTF–CVIA (2.4 μM), compound **1** (20 μM), and PFTase (200 nM). After incubation at room temperature for 90 min, the reaction mixture was analyzed by LC–MS to ensure complete prenylation using the gradient conditions described above.

Simultaneous Coupling Reactions between Bifunctionalized GFP (4) with Azido-bis-methotrexate (bis-MTX) (S14) and Aminooxy-TAMRA (S15) To Yield TAMRA–GFP–Bis-MTX (6). Aminooxy-TAMRA (**S15**) (7 μL of 2.2 mM solution in DMSO) and azide-bis-MTX (**S14**) (7 μL of 10 mM solution in DMSO) were added to 100 μL of compound **4** (stock solution of 40 μM in PB). $CuSO_4$ (1 mM), TCEP (1 mM), TBTA (100 μM), and mPDA (40 mM) were added to the mixture, and the reaction was allowed to proceed for 15 h. LC–MS analysis of the sample using the gradient conditions described above showed >90% conversion of the click reaction and >99% oxime ligation on the bifunctionalized protein **4**. The mixture was then purified using a NAP-5 column to remove the excess reagents.

Chemically Induced Self-Assembly of Dihydrofolate Reductase (DHFR) Proteins by TAMRA–GFP–Bis-MTX (6). To study the self-assembly of dimeric DHFR (DD) proteins by TAMRA–GFP–bis-MTX (**6**), an equimolar mixture of relevant dimeric DHFR protein and compound **6** was mixed and incubated at room temperature for 2 h. Next, the samples were analyzed by size-exclusion chromatography (SEC) for the formation of higher order species using our established high-performance size-exclusion chromatography (HP-SEC) method.[28] Briefly, 100 μL of the incubated sample (10 μM) was injected onto a Superdex G75 size-exclusion column (10 × 300 mm) and eluted with P500 buffer [0.5 M NaCl, 50 mM KH_2PO_4, and 1 mM ethylenediaminetetraacetic acid (EDTA) at pH 7] at 0.5 mL/min. The elution profile was monitored at 280 nm.

Confocal Microscopy. HPB-MLT cells (0.5×10^6) were treated with compound **6** (1 μM) for control experiments and with self-assembled nanostructures at either 4 or 37 °C for 1 h in RPMI media. Cells were then pelleted by centrifugation (400*g* for 5 min). After being washed twice with phosphate-buffered saline (PBS), cells were incubated on Poly-Prep slides coated with poly-L-lysine (Sigma) at 4 or 37 °C for 30 min. Cells were then fixed with 4% paraformaldehyde solution for 10 min and washed 3 times with PBS. Finally, cells were treated with ProLong Gold Antifade reagent with 4′,6-diamidino-2-phenylindole (DAPI) (Invitrogen), and a coverslip was applied. After overnight incubation, they were imaged by fluorescence confocal microscopy using an Olympus FluoView 1000 BX2 upright confocal microscope.

Flow Cytometry. HPB-MLT cells (1×10^6) were treated with self-assembled nanostructures (1, 0.5, and 0.1 μM) at 4 °C for 1 h in PBS buffer [containing 0.05% bovine serum albumin (BSA) and 0.1% sodium azide]. Cells were pelleted (400*g* for 10 min), washed twice, and resuspended in the supplemented PBS, and their fluorescence was analyzed with a FACS Calibur flow cytometer (BD Biosciences). For the positive control experiment, HPB-MLT cells (1×10^6) were incubated with 40 nM fluorescein isothiocyanate (FITC)-labeled UCHT-1 (anti-CD3 monoclonal antibody). After 2 h of incubation, cells were washed, resuspended, and analyzed by flow cytometry. A negative control experiment was performed with self-assembled nanostructures treated with CD3 negative Daudi B lymphoma cells (1×10^6 cells).

RESULTS AND DISCUSSION

Design, Synthesis, and Enzymatic Reaction with a Triorthogonal Protein Labeling Reagent. To obtain site-selective protein labeling, triorthogonal compound **1** was

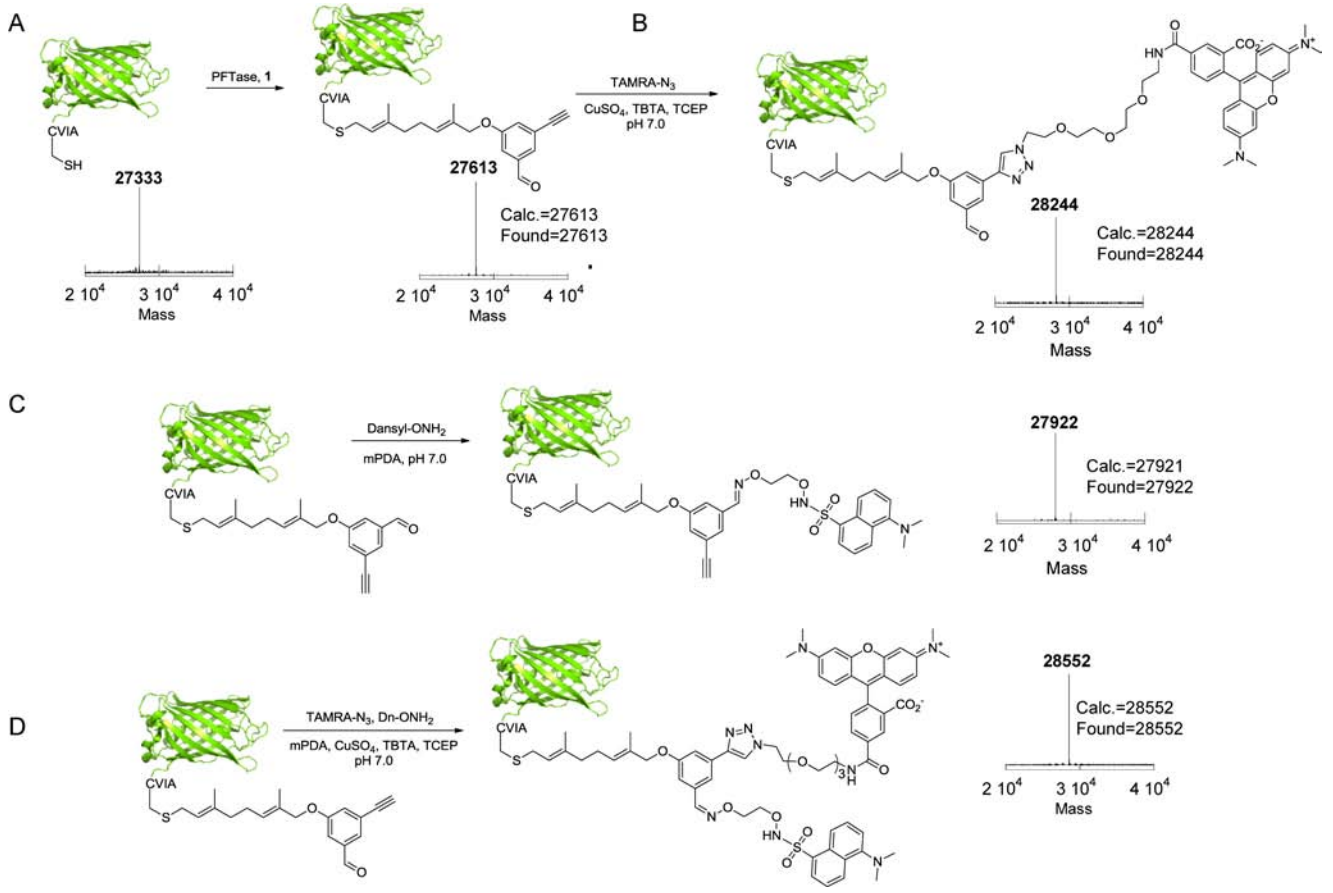

Figure 3. (A) Schematic representation of prenylation of GFP−CVIA (**3**) with FPP analogue **1** to yield bifunctionalized GFP (**4**). The deconvoluted mass spectra are shown adjacent to the compound structures, showing successful prenylation of GFP **3**. (B) Schematic representation of the click reaction between bifunctionalized GFP (**4**) with azido-TAMRA (**S11**) to yield labeled GFP **4a**. The deconvoluted mass spectrum of the clicked product is shown adjacent to the product, showing a successful click reaction between compounds **S11** and **4**. (C) Schematic representation of the oxime ligation reaction between bifunctionalized GFP (**4**) and aminooxy-dansyl (**S10**) to yield oxime GFP **4b**. The deconvoluted mass spectrum is shown adjacent to the oxime product, indicating a successful oxime ligation reaction. (D) Schematic representation of simultaneous click and oxime reactions between bifunctionalized GFP (**4**) with aminooxy-dansyl (**S10**) and azido-TAMRA (**S11**) to yield GFP **4c**. The deconvoluted mass spectrum of the product is shown, showing successful simultaneous click and oxime reactions between compounds **S10**, **S11**, and **4**.

designed. The molecule contains a geranyl substructure including an allylic diphosphate to render it a substrate for PFTase along with aldehyde and alkyne functional groups to allow for two distinct bioorthogonal reactions. Docking of compound **1** into the active site of PFTase indicates that compound **1** can adopt a conformation similar to that of the physiological substrate, FPP (left panel of Figure 2), and that sufficient room exists to accommodate the 1,3,5-trisubstituted aryl ring (right panel of Figure 2). Inspection of the docked structure also suggests that ortho substitution to the phenoxide oxygen could lead to unfavorable steric interactions with the protein. Hence, for wild-type PFTase, the 1,3,5-substitution pattern appears to be the optimal design.

Compound **1** was then synthesized from commercially available geraniol and 3,5-dihydroxybenzaldehyde in nine steps (see Figure S3 of the Supporting Information). In brief, tetrahydropyranyl acetal (THP)-protected geraniol was initially oxidized at C-8 to a terminal alcohol, followed by bromination of the hydroxyl group using CBr_4 and PPh_3. The 3,5-alkyne−aldehyde−functionalized phenol was prepared from 3,5-dihydroxybenzaldehyde via a Sonogashira Pd−Cu-catalyzed cross-coupling reaction[29] in three steps. The modified phenol was alkylated with the aforementioned bromide using K_2CO_3 as the base. The THP group was removed, and the alcohol was converted to the corresponding diphosphate via a direct phosphorylation strategy employing $(HNEt_3)_2HPO_4$ and CCl_3CN as the activating reagent. Subsequent purification by reversed-phase high-pressure liquid chromatography (RP-HPLC) produced the desired bifunctional aldehyde−alkyne analogue **1**, whose structure was confirmed by ^1H nuclear magnetic resonance (NMR), ^{31}P NMR, and high-resolution electrospray ionization mass spectrometry (HR-ESI−MS).

Initially, prenylation reactions containing a model peptide, *N*-dansyl-GCVIA (**2**), analogue **1**, and PFTase were performed, and the reactions were monitored via a continuous fluorescence-based enzyme assay, as previously reported,[30] which demonstrated that compound **1** is an alternative substrate for the enzyme. Next, a kinetic analysis of that reaction was performed using varying concentrations of compound **1** and *N*-dansyl-GCVIA (**2**) in the presence of PFTase, showing that the enzymatic process obeyed saturation kinetics. Steady-state kinetic parameters for the prenylation reaction using the bifunctional aldehyde−alkyne analogue are provided in Figure S4 of the Supporting Information. This analysis revealed that the catalytic efficiency for alternative substrate **1** is reduced relative to that of FPP, with a k_{cat}/K_M

dx.doi.org/10.1021/ja403813b | J. Am. Chem. Soc. 2013, 135, 16388−16396

value of 0.02 (relative to FPP). We found that a decrease in k_{cat} constituted the major reason for the diminished catalytic activity with the analogue, with the k_{cat} value for compound **1** (k_{cat} = 0.0123 s^{-1}) observed to be 42-fold lower than the k_{cat} for FPP (k_{cat} = 0.52 s^{-1}), while no substantial difference was observed between the K_M values for the analogue (K_M = 2.52 μM) and FPP (K_M= 1.71 μM). It should be noted that, while the docking results shown above (left panel of Figure 2) suggest that compound **1** binds in a conformation similar to that of FPP, small differences are apparent in the vicinity of C-1 of the isoprenoid and the diphosphate, which may account for the reduced reactivity. Nevertheless, despite this lower activity with compound **1**, using elevated levels of PFTase (200 nM), it is relatively easy to drive these enzymatic reactions to completion in 2 h.

Application of Triorthogonal Protein Labeling to an Individual Protein. With the ability of analogue **1** to be incorporated by PFTase established, we next evaluated the utility of the analogue for selective protein modification. Accordingly, compound **1** was incubated with GFP−CVIA (**3**) in the presence of PFTase (4 h at room temperature). That choice of reaction time was based on our earlier work with the peptide substrate *N*-dansyl-GCVIA (**2**), where a 2 h reaction resulted in complete conversion. Concentration by ultracentrifugation followed by SEC to remove excess compound **1** yielded pure bifunctionalized GFP (**4**) (Figure 3A). Completion of the reaction was confirmed by LC−ESI−MS, with the major peak corresponding to prenylated GFP (**4**) and a minor peak corresponding to a negligible amount of unreacted GFP−CVIA (**3**) (Figure 3A).

In previous studies, we had shown that aldehyde−GFP- and alkyne−GFP-modified proteins could be derivatized to produce oxime-linked or clicked products, respectively.[23,27] In this study, we explored simultaneous oxime and click reactions on a single prenylated protein. First, to demonstrate the orthogonality of the two reactions, a separate oxime ligation or click reaction was carried out with the bifunctionalized protein. Thus, oxime ligation on compound **4** was performed with an aminooxy-dansyl reagent (**S10**) using mPDA as the catalyst.[31] LC−MS analysis of the crude ligation reaction mixture confirmed complete conversion to the oxime-linked product **4b** in less than 1 h (Figure 3C). The click reaction was tested on compound **4** with azido-TAMRA (**S11**) using TCEP, TBTA, and copper as the catalyst to yield GFP−TAMRA **4a** (Figure 3B). LC−MS analysis revealed that >80% conversion was obtained within 12 h of reaction, using equimolar concentrations of prenylated protein and the coupling partner (azido-TAMRA, **S11**) as used in the above oxime ligation reaction (Figure 3B). Typically, the oxime ligation reaction proved to be modestly more efficient than the click reaction. When the oxime and click reactions were carried out simultaneously on the modified protein to yield **4c** using equimolar concentrations of reagents (*vide supra*), quantitative conversion for the oxime reaction and ∼90% conversion for the click reaction after 12 h were observed (Figure 3D).

After optimizing the conditions for the oxime and click reactions on the bifunctional prenylated protein **4**, we next evaluated the preparation of a PEG−GFP−TAMRA (**4d**) (Figure 4A). We chose TAMRA and PEG as examples because fluorophore can act as a biophysical or cellular localization tool, while PEG can improve protein pharmacokinetics. Protein **4** was incubated first with azido-TAMRA (**S11**) under the optimized click reaction conditions described above for 12 h.

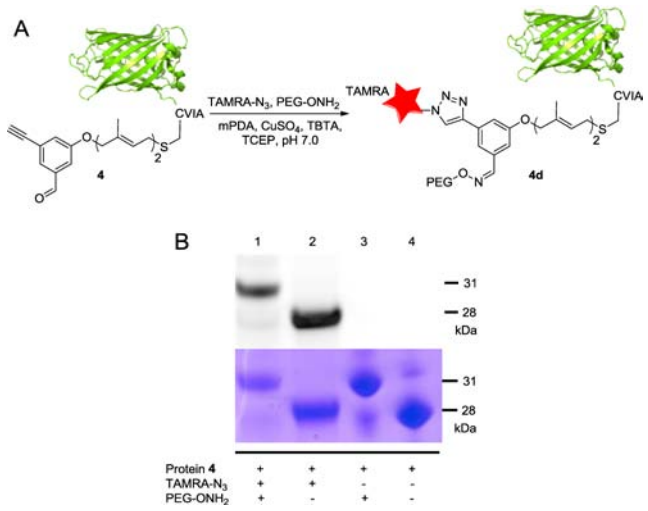

Figure 4. (A) Schematic representation of oxime ligation and click reaction of the bifunctionalized prenylated protein **4** with aminooxy-PEG (3 kDa) (**S12** and azido-TAMRA (**S11**) followed by analysis of the reactions via SDS−PAGE. (B) SDS−PAGE analysis of the aforementioned click and oxime reactions. Densitometry analysis on the SDS−PAGE of the aforementioned reactions revealed highly selective and almost complete (>95%) conversions for both oxime and click reactions on the prenylated protein. The lower bands were visualized by staining with Coomassie Blue, while the upper bands were detected via in-gel fluorescence imaging of TAMRA. Lane 1, reaction mixture containing protein **4**, PEG−ONH_2, and TAMRA−N_3; lane 2, reaction mixture containing protein **4** and TAMRA−N_3; lane 3, reaction mixture containing protein **4** and PEG−ONH_2; and lane 4, solution containing only protein **4**. Densitometry analyses were performed using ImageJ, version 1.46.

LC−MS analysis on the reaction mixture revealed complete conversion of bifunctionalized protein **4** to GFP−TAMRA (**4a**). Subsequently, the product was incubated with aminooxy-PEG (3 kDa) (**S12**, from Quanta BioDesign) at pH 7 in the presence of mPDA (40 mM) as a catalyst for 2 h. SDS−PAGE analysis of the aforementioned reactions revealed highly selective and almost complete (>95%) conversions for both oxime and click reactions with the prenylated protein (Figure 4). The lower bands (Figure 4B) were visualized by staining with Coomassie Blue, while the upper bands were detected via in-gel fluorescence imaging of TAMRA. That data showed that the reaction mixture including protein **4**, aminooxy-PEG, and azido-TAMRA contained a species with lower mobility in the SDS−PAGE gel because of the higher mass obtained upon addition of the PEG group; a dark band was also observed via in-gel fluorescence imaging of TAMRA (lane 1 in Figure 4B) that comigrated with the lower mobility species noted above. When no PEG reagent was present in the reaction mixture, the lower mobility band was absent (lane 3 in Figure 4B), and when azido-TAMRA was not present in the reaction, only the higher mobility species that migrated near the starting protein was fluorescently labeled. Taken together, these results establish that two different functionalities can be installed simultaneously into a protein via two distinct bioorthogonal reactions using this triorthogonal labeling strategy.

Application of Triorthogonal Protein Labeling to a Protein of Biomedical Importance. Having established the utility of this method for C-terminal site-specific modification with a model protein, GFP, we decided to illustrate its use by modifying a biomedically important protein. CNTF is a

dx.doi.org/10.1021/ja403813b | J. Am. Chem. Soc. 2013, 135, 16388−16396

member of a class of proteins that promote neuron survival during inflammatory events and can stimulate neurite outgrowth.[32] Recently, CNTF has been studied extensively as a possible therapeutic agent for slowing retinal degeneration.[33,34] Thus, we elected to investigate the preparation of a bifunctionalized CNTF using the new strategy reported here. To accomplish this, purified CNTF−CVIA (**5**),[31] a form of CNTF engineered to contain a C-terminal CaaX box, was prenylated with analogue **1** followed by labeling using azido-TAMRA (**S11**) and PEGylation with aminooxy-PEG (**S13**). LC−MS analysis (Figure 5) confirmed successful prenylation and subsequent modification of CNTF by both azido-TAMRA (**S11**) and aminooxy-PEG (**S13**).

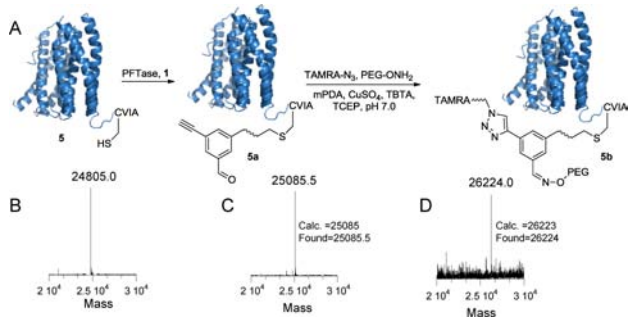

Figure 5. (A) Prenylation of CNTF−CVIA (**5**) with FPP analogue **1** followed by simultaneous fluorophore labeling and PEGylation of the prenylated protein **5a** via click and oxime ligations with azido-TAMRA (**S11**) and aminooxy-PEG (**S13**) to yield compound **5b**. (B−D) Deconvoluted mass spectra are shown, showing successful prenylation (B, pure CNTF; C, prenylated CNTF) and simultaneous click and oxime reactions (D).

Application of the Triorthogonal-Protein-Labeling Reagent in Macromolecular Protein Self-Assembly (Figure 7). Self-organization of protein molecules into higher order structures is an integral part of living cells. Unlike DNA- and RNA-based nanostructures,[35−38] the rules governing protein self-assembly are only beginning to be defined. Much of the previous effort to construct biomimetic protein assemblies has been based on direct protein−protein interactions through the incorporation of complementary amino acid residue surface interactions.[39] As an alternative, chemical biological approaches for macromolecular protein assembly based on metal coordination,[40] polymer conjugation,[41] enzyme−inhibitor interactions,[42−44] and chemically induced dimerization[45] have begun to be explored.

In previous work, we reported on the design of chemically self-assembled nanoring structures (CSANs) constructed from dimeric forms of DHFR and bis-MTX.[46] Upon mixing, the two components spontaneously assemble into a mixture of compact rings and polymeric structures that can be readily separated by SEC. The ring structures have been studied by dynamic light scattering, transmission electron microscopy (TEM), and atomic force microscopy (AFM), and it has been shown that the number of DHFR and MTX dimers in the ring can be controlled by the length of the linker region that joins the two DHFR monomers; because of the high affinity of MTX for DHFR and, thus, high effective molarity, the cyclic forms resist linearization in the absence of an exogenous inhibitor of DHFR.[46,47] The CSANs are highly stable exhibiting T_m values between 62 and 65 °C (unpublished observation). The utility of the nanorings has been expanded to incorporate single-chain antibodies (scFvs) and peptides, thus allowing them to be targeted to cell surface receptors. In particular, we have previously demonstrated that anti-CD3 scFv−DHFR[2] fusion proteins containing a 13 amino acid linker or a 1 amino acid linker will self-assemble in the presence of a bis-MTX into bi- and octavalent anti-CD3 CSANs, respectively. Further, we have demonstrated that the anti-CD3 CSANs bind specifically to $CD3^+$ T-leukemia cells with dissociation constants comparable to the parental monoclonal antibody (UCHT-1 mAb, K_d = 1.8 nM; bivalent anti-CD3 CSANs, K_d = 3.5 nM; and octavalent anti-CD3, K_d = 0.93 nM). In addition, the anti-CD3 CSANs undergo rapid clathrin-dependent endocytosis by T-leukemia cells, which enables drug or oligonucleotide delivery.[28,47−49] To demonstrate the ability of the CSANs to carry out protein delivery, we decided to explore the use of the dual-labeling strategy reported here to link the bis-MTX element to a protein. Accordingly, we designed and prepared anti-CD3-CSANs capable of delivering a protein cargo into T-leukemia cells. Thus, bis-MTX−GFP−TAMRA (**6**) was prepared. A previously reported amino-bis-MTX trilinker[48] (**S16**) was coupled to 5-azidopentanoic acid using standard peptide chemistry to obtain azido-bis-MTX (**S14**). Next, the bifunctional prenylated protein **4** described above was incubated with aminooxy-TAMRA (**S15**) and azido-bis-MTX (**S14**) for 15 h using the optimized reaction conditions (*vide supra*). Subsequent LC−MS analysis of the reaction mixture revealed the successful simultaneous conjugation of the protein with both aminooxy-TAMRA and azido-bis-MTX (Figure 6).

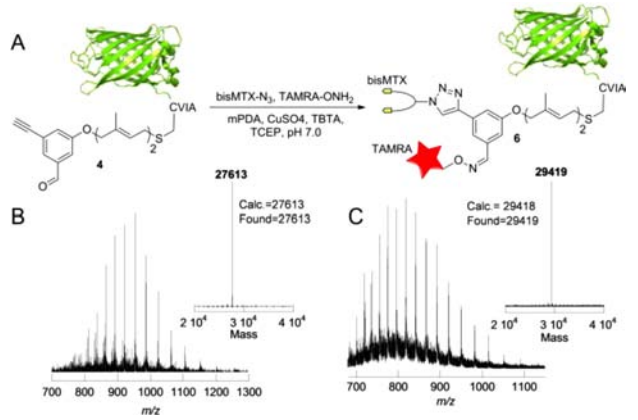

Figure 6. (A) Schematic representation of simultaneous oxime ligation and click reactions of the bifunctionalized prenylated protein **4** with azido-bis-MTX (**S14**) and aminooxy-TAMRA (**S15**). (B and C) ESI−MS analysis of compounds **4** and **6** with the deconvoluted mass spectra shown in the insets, respectively.

Overall, the conjugation reactions appear to be highly efficient, because little free starting material was observed by LC−MS; the high efficiency seen in this case is similar to results noted above for other GFP and CNTF conjugates. With the bis-MTX- and TAMRA-functionalized GFP protein **6** in hand, we then evaluated the chemically induced self-assembly of this protein with dimeric DHFR (DD) proteins by HP-SEC. After simple mixing of the two entities and incubation at room temperature for 2 h, the samples were analyzed by HP-SEC. The elution profiles of the HP-SEC chromatograms indicated the predominant formation of the internal monomeric species with 13-DHFR−DHFR (13DD) and a much higher order species with 1-DHFR−DHFR (1DD; see Figures S10 and S11

dx.doi.org/10.1021/ja403813b | J. Am. Chem. Soc. 2013, 135, 16388−16396

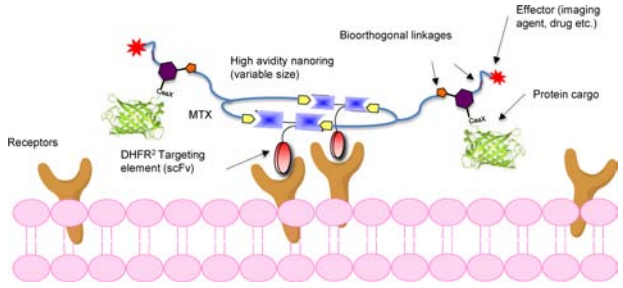

Figure 7. Application of the dual protein-labeling strategy in macromolecular protein self-assembly. A high-avidity "effector–antibody–fluorophore" conjugate for therapeutic cargo delivery and tracking was designed and synthesized.

of the Supporting Information). Note that, in this nomenclature system, 13DD is a single polypeptide chain incorporating two DHFR domains separated by a 13 residue spacer, whereas 1DD is a similar dimer separated by a 1 residue spacer.[28] Having confirmed the self-assembly with non-targeting DHFR proteins, we then moved to construct the TAMRA–GFP–DD–anti-CD3 protein nanostructures by mixing 13DD-anti-CD3 (13DDCD3) and 1DD-anti-CD3 (1DDCD3) with compound **6**. These latter DHFR-based constructs are similar to 13DD and 1DD, with the exception that they each have a single-chain antibody (anti-CD3) fused to the C terminus of the DHFR dimer; the presence of the anti-CD3 moiety allows these constructs to be targeted to cells displaying the CD3 antigen. The assemblies containing the targeting proteins generated a similar pattern in the SEC profile compared to the constructs prepared from DHFR dimers lacking the anti-CD3 domain (Figure 8).

Consistent with what was observed with the corresponding non-targeting DHFR proteins, TAMRA–GFP–DDCD3 CSANs prepared with 13DDCD3 (**7**) exhibited predominantly internal monomer, dimers, and small amounts of higher order species. The species eluting between 20 and 22.5 min (**7**) were

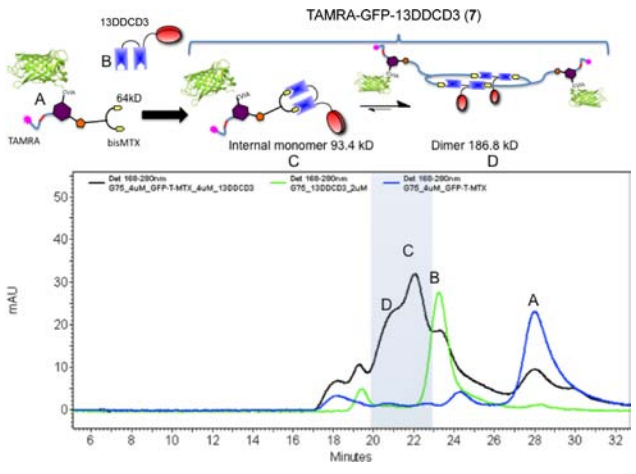

Figure 8. Self-assembly of antibody nanorings **7** observed by SEC (13DDCD3 with compound **6**). Blue curve, bis-MTX–GFP–TAMRA (**6**, peak A); green curve, monomeric 13DDCD3 (peak B); black curve, induced oligomerization of 13DDCD3 with compound **6** indicating the major products as the internal monomer (peak C) and dimer (peak D). The shaded area indicates the material collected and used for subsequent biological studies. HP-SEC was performed using a Superdex G75 column with a flow rate of 0.5 mL/min and monitoring at 280 nm.

collected and concentrated by ultrafiltration, and their final concentration was determined on the basis of the collected peak area. This material was used for cellular internalization studies (Figure 9). Similar SEC experiments and cell internalization experiments were performed with assemblies prepared from 1DDCD3 as well, which gave similar results to those obtained with 13DDCD3 (see Figure S12 of the Supporting Information for SEC data and Figures S13 and S14 of the Supporting Information for cell experiments).

To study the functionality of the TAMRA–GFP–13DDCD3 and TAMRA–GFP–1DDCD3 CSANs (**7** and **8**, respectively), we evaluated their ability to specifically deliver the protein nanostructure to $CD3^+$ T-leukemia cells. The cells were incubated with compound **7** for 1 h (at 4 and 37 °C) and evaluated by confocal laser scanning microscopy for cellular internalization. Both the GFP and TAMRA chromophores were excited individually to observe the GFP and TAMRA emission. Additionally, FRET was observed between the two fluorophores when GFP was excited and TAMRA emission was monitored. First, control experiments in which $CD3^+$ T-leukemia cells were treated only with the GFP–TAMRA conjugate **6** showed minimal fluorescence (Figure 9G). In addition, no significant binding to $CD3^+$ T-leukemia cells by CSANs prepared with compound **6** was observed by FACS (see Figure S15 of the Supporting Information) Confocal microscopy imaging confirmed the delivery of the nanostructures (**7** and **8**) into the cells via an energy-dependent endocytic process (Figure 9 and Figures S12–S14 of the Supporting Information). At 4 °C, TAMRA fluorescence was observed on the cell membranes (Figure 9A), and at 37 °C, distinct punctate structures (Figure 9B) were observed within the cells, indicating the energy-dependent uptake of both GFP and TAMRA. Overlay of the GFP/TAMRA channels indicated that the two fluorophores were present in the same location (Figure 9H), while the positive FRET signal was consistent with the GFP–TAMRA conjugate **6** having remained intact in the cells during the time period of the experiment (24 h) (panels I and J of Figure 9). The observed temperature-dependent uptake of nanostructures at 37 °C and the punctate structures are consistent with our previous observations with anti-CD3 scFv CSANs.[28]

As was noted in earlier studies with anti-CD3 CSANs, flow cytometric analysis (see Figures S15 and S16 of the Supporting Information) revealed that the nanostructure binds specifically to $CD3^+$ HPB-MLT cells but not $CD3^-$ Daudi cells (see Figure S19 of the Supporting Information). When compared, little difference by flow cytometry was observed between the binding by CSANs prepared from 13DDCD3 (**7**) and 1DDCD3 (**8**) to $CD3^+$ HPB-MLT cells (Figure 10 and Figures S17 and S18 of the Supporting Information).

■ CONCLUSION

In summary, we have designed a triorthogonal reagent to site-specifically modify a protein with two orthogonal groups that can be subsequently functionalized in a single one-pot procedure. Our approach relies on the selective tagging of proteins containing an appended farnesyl transferase substrate sequence. The incorporation of the bifunctional ethynyl-hydroxybenzaldehyde into the farnesyl group facilitates the facile labeling of proteins with two different moieties, thus expanding the potential capabilities of the tagged protein. The simultaneous tagging of the cytokine, CNTF, with PEG and a fluorophore, suggests that the alteration and monitoring of the

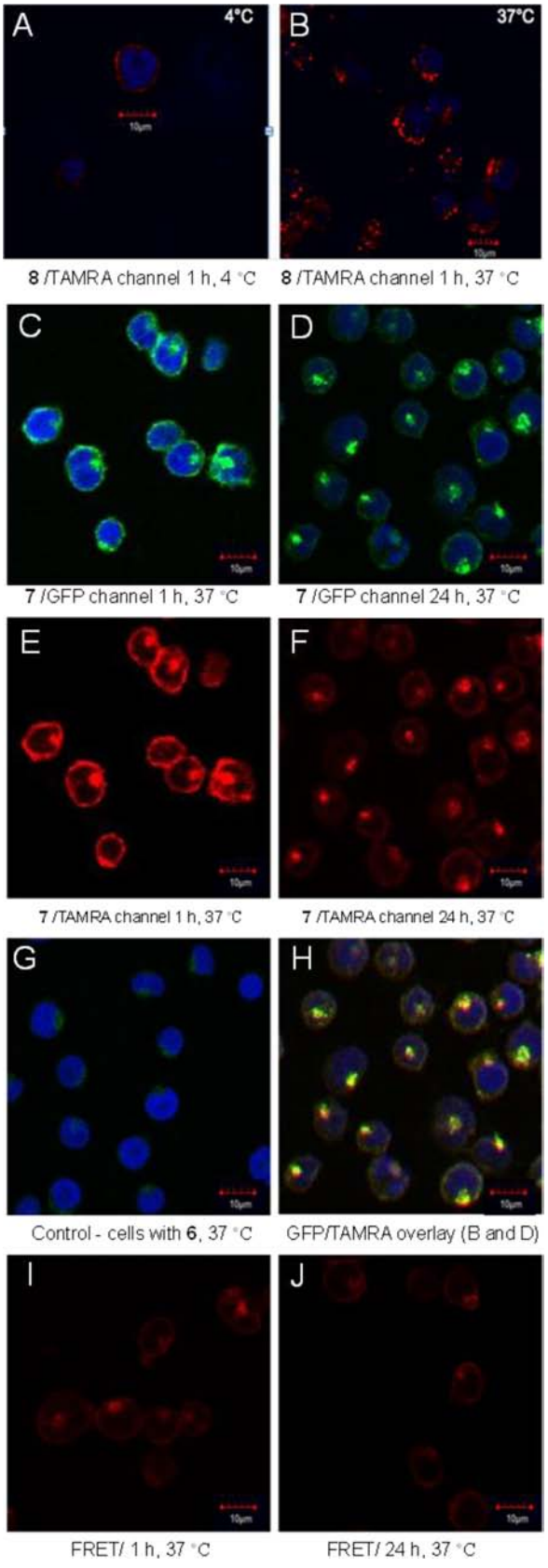

Figure 9. (A and B) Internalization studies of TAMRA−GFP−1DDCD3 (**8**) with HPB-MLT T-leukemia cells at either (left) 4 °C or (right) 37 °C. Cells were treated for 1 h. Images indicate red punctate structures (left) on the cell membrane at 4 °C or (right) within the cell at 37 °C (TAMRA channel). Magnification = 60×. (C−J) Internalization studies of TAMRA−GFP−13DDCD3 (**7**) with HPB-MLT T-leukemia cells at 37 °C: (C and E) compound **7** incubated with $CD3^+$ T-leukemia cells for 1 h (C, DAPI and GFP channels; E, TAMRA channel), (D and F) compound **7** incubated with $CD3^+$ T-leukemia cells for 24 h (D, DAPI and GFP channels; F, TAMRA channel), (G) HPB-MLT cells treated with bis-MTX−GFP−TAMRA (**6**) for 1 h (control; blue = DAPI nuclear stain), (H) overlay of the GFP and TAMRA channels indicating the intact assembled protein (co-localized yellow punctate), and (I and J) FRET between GFP and TAMRA observed by exciting the cells with 488 nm laser and a BA560/620 nm emission filter.

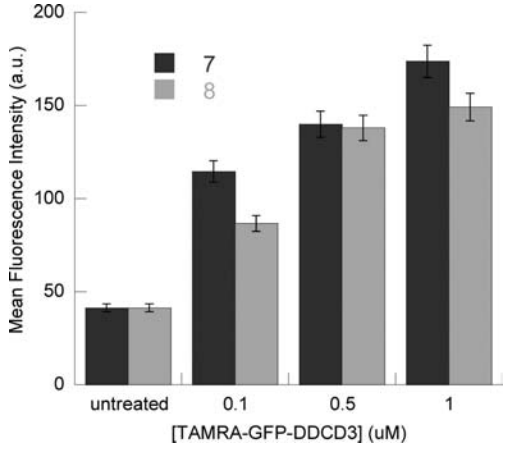

Figure 10. Determination of the dose-dependent CD3 receptor binding of assembled protein nanostructures and comparison of the TAMRA−GFP−13DDCD3 (**7**) and TAMRA−GFP−1DDCD3 (**8**) bindings using mean fluorescence values obtained from the TAMRA channel. HPB-MLT cells were treated with different concentrations of self-assembled nanostructures, **7** or **8**, at 37 °C for 1 h before flow cytometry analysis. For the FACS measurements, 10 000 cells were counted for each sample and the average mean fluorescence intensity from three replicates is plotted here along with the standard error (indicated by the error bars).

biodistribution properties and pharmacokinetic behavior of a potential therapeutic protein can be easily coupled. In addition, we have demonstrated that this approach can be used to direct the assembly of protein complexes while monitoring their interactions with cells. Future studies will examine the ability of our trifunctional bioconjugation approach to enhance the plasma half-life of CaaX-box PEGylated proteins by simultaneously monitoring their tissue distribution with an appended fluorophore or radiolabel. It should also be possible to combine the method reported here with other strategies, noted above,[15−18] for bioorthogonal protein labeling to further tailor the properties of proteins or create more complex constructs thereof.

■ ASSOCIATED CONTENT

Ⓢ Supporting Information

Detailed experimental procedures for synthesis of compound **1**, enzymatic studies of FPP analogue **1** as a substrate for PFTase, synthesis of azido-bis-MTX (**S14**), and confocal microscopy and flow cytometry images. This material is available free of charge via the Internet at http://pubs.acs.org.

dx.doi.org/10.1021/ja403813b | J. Am. Chem. Soc. 2013, 135, 16388−16396

AUTHOR INFORMATION

Corresponding Authors

wagne003@umn.edu
diste001@umn.edu

Author Contributions

[†]Mohammad Rashidian and Sidath C. Kumarapperuma contributed equally to this work.

Notes

The authors declare no competing financial interest.

ACKNOWLEDGMENTS

Financial support for these studies through National Institutes of Health (NIH) Grants GM058842 (to Mark D. Distefano), GM084152 (to Mark D. Distefano), and CA120116 (to Carston R. Wagner) and the University of Minnesota is gratefully acknowledged.

REFERENCES

(1) Bertozzi, C. R. *Acc. Chem. Res.* **2011**, *44*, 651−653.
(2) Prescher, J. A.; Bertozzi, C. R. *Nat. Chem. Biol.* **2005**, *1*, 13−21.
(3) Mamidyala, S. K.; Finn, M. G. *Chem. Soc. Rev.* **2010**, *39*, 1252.
(4) Christman, K. L.; Broyer, R. M.; Tolstyka, Z. P.; Maynard, H. D. *J. Mater. Chem.* **2007**, *17*, 2021.
(5) Prost, L. R.; Grim, J. C.; Tonelli, M.; Kiessling, L. L. *ACS Chem. Biol.* **2012**, *7*, 1603−1608.
(6) Wang, T.; Kartika, R.; Spiegel, D. A. *J. Am. Chem. Soc.* **2012**, *134*, 8958−8967.
(7) Park, S.; Yousaf, M. N. *Langmuir* **2008**, *24*, 6201−6207.
(8) Keppler, A.; Pick, H.; Arrivoli, C.; Vogel, H.; Johnsson, K. *Proc. Natl. Acad. Sci. U. S. A.* **2004**, *101*, 9955−9959.
(9) Yin, J.; Liu, F.; Li, X.; Walsh, C. T. *J. Am. Chem. Soc.* **2004**, *126*, 7754−7755.
(10) Chen, I.; Ting, A. Y. *Curr. Opin. Biotechnol.* **2005**, *16*, 35−40.
(11) Discher, D. E.; Eisenberg, A. *Science* **2002**, *297*, 967−973.
(12) Kim, C. H.; Axup, J. Y.; Dubrovska, A.; Kazane, S. A.; Hutchins, B. A.; Wold, E. D.; Smider, V. V.; Schultz, P. G. *J. Am. Chem. Soc.* **2012**, 9918−9921.
(13) Hudak, J. E.; Barfield, R. M.; de Hart, G. W.; Grob, P.; Nogales, E.; Bertozzi, C. R.; Rabuka, D. *Angew. Chem., Int. Ed.* **2012**, *51*, 4161−4165.
(14) Witte, M. D.; Cragnolini, J. J.; Dougan, S. K.; Yoder, N. C.; Popp, M. W.; Ploegh, H. L. *Proc. Natl. Acad. Sci. U. S. A.* **2012**, *109*, 11993−11998.
(15) Yi, L.; Sun, H.; Itzen, A.; Triola, G.; Waldmann, H.; Goody, R. S.; Wu, Y.-W. *Angew. Chem., Int. Ed. Engl.* **2011**, *50*, 8287−8290.
(16) Brustad, E. M.; Lemke, E. A.; Schultz, P. G.; Deniz, A. A. *J. Am. Chem. Soc.* **2008**, *130*, 17664−17665.
(17) Kim, J.; Seo, M.-H.; Lee, S.; Cho, K.; Yang, A.; Woo, K.; Kim, H.-S.; Park, H.-S. *Anal. Chem.* **2013**, *85*, 1468−1474.
(18) Feng, L.; Hong, S.; Rong, J.; You, Q.; Dai, P.; Huang, R.; Tan, Y.; Hong, W.; Xie, C.; Zhao, J.; Chen, X. *J. Am. Chem. Soc.* **2013**, *135*, 9244−9247.
(19) Rashidian, M.; Dozier, J. K.; Lenevich, S.; Distefano, M. D. *Chem. Commun.* **2010**, *46*, 8998.
(20) Weinrich, D.; Lin, P.-C.; Jonkheijm, P.; Nguyen, U. T. T.; Schröder, H.; Niemeyer, C. M.; Alexandrov, K.; Goody, R.; Waldmann, H. *Angew. Chem., Int. Ed.* **2010**, *49*, 1252−1257.
(21) Gauchet, C.; Labadie, G. R.; Poulter, C. D. *J. Am. Chem. Soc.* **2006**, *128*, 9274−9275.
(22) Kim, M.; Kleckley, T. S.; Wiemer, A. J.; Holstein, S. A.; Hohl, R. J.; Wiemer, D. F. *J. Org. Chem.* **2004**, *69*, 8186−8193.
(23) Rashidian, M.; Song, J. M.; Pricer, R. E.; Distefano, M. D. *J. Am. Chem. Soc.* **2012**, *134*, 8455−8467.
(24) Placzek, A. T.; Gibbs, R. A. *Org. Lett.* **2011**, 3576−3579.
(25) Labadie, G. R.; Viswanathan, R.; Poulter, C. D. *J. Org. Chem.* **2007**, *72*, 9291−9297.
(26) Subramanian, T.; Liu, S.; Troutman, J. M.; Andres, D. A.; Spielmann, H. P. *ChemBioChem* **2008**, *9*, 2872−2882.
(27) Duckworth, B. P.; Xu, J.; Taton, T. A.; Guo, A.; Distefano, M. D. *Bioconjugate Chem.* **2006**, *17*, 967−974.
(28) Li, Q.; So, C. R.; Fegan, A.; Cody, V.; Sarikaya, M.; Vallera, D. A.; Wagner, C. R. *J. Am. Chem. Soc.* **2010**, *48*, 17247−17257.
(29) Sonogashira, K. *J. Organomet. Chem.* **2002**, *653*, 46−49.
(30) Pompliano, D. L.; Gomez, R. P.; Anthony, N. J. *J. Am. Chem. Soc.* **1992**, *114*, 7945−7946.
(31) Rashidian, M.; Mahmoodi, M. M.; Shah, R.; Dozier, J. K.; Wagner, C. R.; Distefano, M. D. *Bioconjugate Chem.* **2013**, *24*, 333−342.
(32) Ip, N. Y.; Yancopoulos, G. D. *Annu. Rev. Neurosci.* **1996**, *19*, 491−515.
(33) Rhee, K. D.; Yang, X.-J. *Adv. Exp. Med. Biol.* **2010**, *664*, 647−654.
(34) Wen, R.; Tao, W.; Li, Y.; Sieving, P. A. *Prog. Retinal Eye Res.* **2012**, *31*, 136−151.
(35) Rothemund, P. W. K. *Nature* **2006**, *440*, 297−302.
(36) Pistol, C.; Dwyer, C. *Nanotechnology* **2007**, *18*, 125305.
(37) Guo, P. *Nat. Nanotechnol.* **2010**, *5*, 833−842.
(38) Ke, Y.; Lindsay, S.; Chang, Y.; Liu, Y.; Yan, H. *Science* **2008**, *319*, 180−183.
(39) Matsuura, K.; Watanabe, K.; Matsuzaki, T.; Sakurai, K.; Kimizuka, N. *Angew. Chem., Int. Ed.* **2010**, *49*, 9662−9665.
(40) Salgado, E. N.; Radford, R. J.; Tezcan, F. A. *Acc. Chem. Res.* **2010**, *43*, 661−672.
(41) Hu, M.; Qian, L.; Briñas, R. P.; Lymar, E. S.; Hainfeld, J. F. *Angew. Chem., Int. Ed. Engl.* **2007**, *46*, 5111−5114.
(42) Chen, G.; Jiang, M. *Chem. Soc. Rev.* **2011**, *40*, 2254.
(43) Uhlenheuer, D. A.; Petkau, K.; Brunsveld, L. *Chem. Soc. Rev.* **2010**, *39*, 2817.
(44) Lai, J. R.; Fischbach, M. A.; Liu, D. R.; Walsh, C. T. *J. Am. Chem. Soc.* **2006**, *128*, 11002−11003.
(45) Fegan, A.; White, B.; Carlson, J. C. T.; Wagner, C. R. *Chem. Rev.* **2010**, *110*, 3315−3336.
(46) Carlson, J. C. T.; Jena, S. S.; Flenniken, M.; Chou, T.; Siegel, R. A.; Wagner, C. R. *J. Am. Chem. Soc.* **2006**, *128*, 7630−7638.
(47) Li, Q.; Hapka, D.; Chen, H.; Vallera, D. A.; Wagner, C. R. *Angew. Chem., Int. Ed.* **2008**, *47*, 10179−10182.
(48) Fegan, A.; Kumarapperuma, S. C.; Wagner, C. R. *Mol. Pharmaceutics* **2012**, *9*, 3218−3227.
(49) Gangar, A.; Fegan, A.; Kumarapperuma, S. C.; Wagner, C. R. *J. Am. Chem. Soc.* **2012**, *134*, 2895−2897.
(50) Viault, G.; Dautrey, S.; Maindron, N.; Hardouin, J.; Renard, P.-Y.; Romieu, A. *Org. Biomol. Chem.* **2013**, *11*, 2693−2705.

NOTE ADDED IN PROOF

After this paper was published ASAP October 17, 2013, it was brought to our attention that, recently, heterotrifunctional molecules that can be incorporated by non-enzymatic methods have also been reported.[50]